Electronic Supplementary Material (ESI) for Journal of Materials Chemistry A.

Supporting Information

Thin and robust organic solvent cation exchange membranes for ion separation

Yan Zhao,[a] Yi Li,[a] Jiajie Zhu,[b] Amaia Lejarazu-Larrañaga,[a, c] Shushan Yuan,[a] Emily Ortega[a],[d] Jiangnan Shen* [b] Congjie Gao,[b] Bart Van der Bruggen* [a]

[a]Department of Chemical Engineering, KU Leuven, Celestijnenlaan 200F, B-3001 Leuven, Belgium.

[b]Center for Membrane Separation and Water Science & Technology, Ocean College, Zhejiang University of Technology, Hangzhou 310014, P. R. China

[c]IMDEA Water institute, Avenida Punto Com 2, Parque Científico Tecnológico de la Universidad de Alcalá, 28805 Alcalá de Henares (Madrid), Spain.

[d] Department of Biological Sciences, University of Wisconsin-Milwaukee, Milwaukee, WI, 53201, United States.

*Corresponding author: Shenjn@zjut.edu.cn
Bart.vanderbruggen@kuleuven.be

This PDF file includes:

Texts S1 to S5

Figure S1 to Figure S12

Table S1 to S11

References (21)

Content

1. Theories 3

1.1. The reactions of dissolved the Kevlar aramid nanofibers. 3
1.2. Amide condensation reaction. 4
1.3. The theory of separation factor. 4

2. Materials 6

3. Methods 7

3.1. Preparation of membrane casting solution. 7
3.2. Preparation of the Kevlar cation exchange membranes. 8
3.3. Measurement of ion exchange capacity of membranes. 8
3.4. Measurement of water content of membranes. 9
3.5. Measurement of swelling rate of membranes. 9
3.6. Measurement of membrane surface electric resistance 9
3.7. Measurement of the membrane zeta potential. 10
3.8. Measurement of the current-voltage curves of all the Kevlar CEMs. 11
3.9. Total reflectance Fourier transforms infrared (ATR-FTIR). 11
3.10. Scanning electronic microscopy (SEM) 11
3.11. X-ray photo-electron spectroscopy (XPS). 11
3.12. The mechanical properties of the membrane. 11
3.13. Desalination of the membranes 12
3.14. Organic solvent property measurement. 13

4. Results 14

4.1. Attenuated total reflectance Fourier transform infrared spectroscopy. 14
4.2. X-ray photoelectron spectroscopy 15
4.3. Polarization current-voltage curves. 16
4.4. Scanning electronic microscopy of membrane surface. 17
4.5. Desalination. 18
4.6. The equation of liner fit for Kevlar CEMs in desalination. 19
4.7. The equation of liner fit for Kevlar CEMs in desalination after measuring the organic solvent property. 20

5. References 21

1. Theories

1.1. The reactions of dissolved the Kevlar aramid nanofibers.

Kevlar is synthesized from poly(p-phenylene terephthalamide) (PPTA) (Fig. S1a), which is the highly asymmetric alternate structure of long molecular chains, and the intermolecular hydrogen bonds between the PPTA molecular chains (Fig. S1b).

The Kevlar aramid nanofiber chains are constituted by the PPTA chains via π-π stacking, van der Waals forces and hydrogen bonds. Before preparation of the Kevlar membrane casting solution, these interactions should be split into polymers by dissolving into DMSO and KOH mixture solution for several days. After that, the long PPTA should be split the amide bond and formed in a nanoscale state (Fig. S1c).

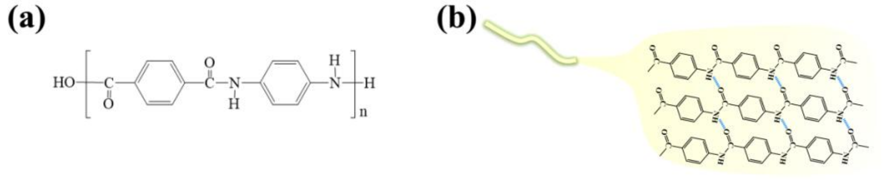

Poly(p-phenylene terephthalamide)

Kevlar aramid nanofibers

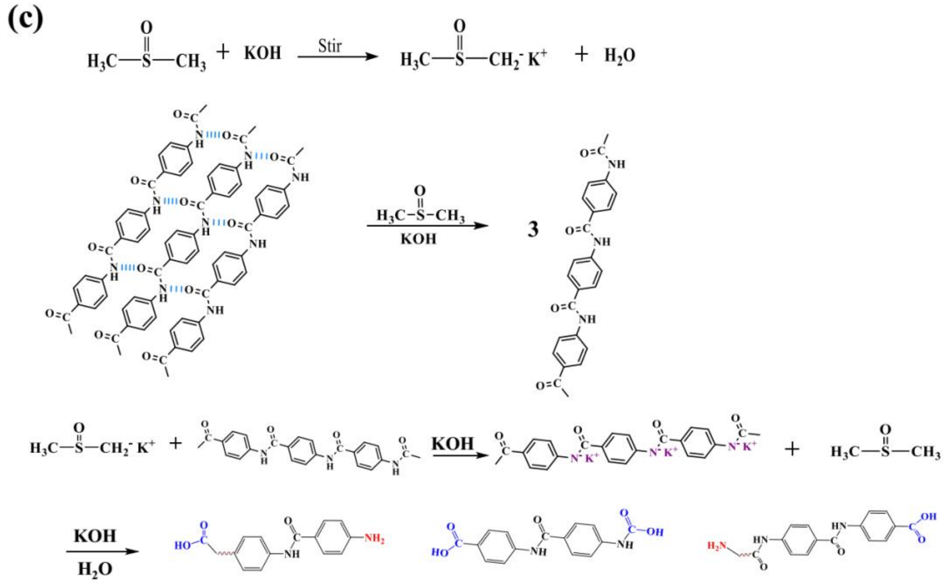

Fig. S1 Chemical structure of poly(p-phenylene terephthalamide) (a); Chemical structure of Kevlar aramid nanofiber (b); The reactions of dissolved the Kevlar aramid nanofibers and formed the poly(p-phenylene terephthalamide) membrane casting (c).

1.2. Amide condensation reaction.

The large number of carboxyl groups (-COOH) in the final PPTA casting solution and lots of amino groups ($-NH_2$) in the 4-amino-benzenesulfonic acid (ABS) monomers. Thus, the amide condensation reaction was reacted between PPTA and ABS under the catalyst of 1-ethyl-3-(3-dimethylami-nopropyl) carbodiimide hydrochloride (EDC-HCl) and N-hydroxy-succinimide (NHS), as shown in Fig. S2.The amide condensation reaction is the negatively charged ABS, which with amount of sulfonic acid groups ($-SO_3H$), were grafted on the PPTA chain sides by chemical bond (-NH-OC-).

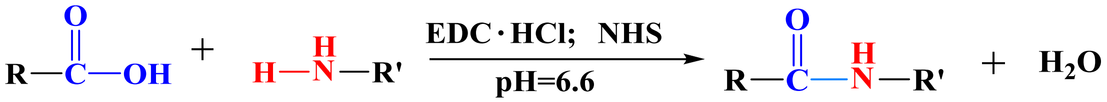

Fig. S2. The amide condensation reaction.

1.3. The theory of separation factor.

The separation factors, which are the solution conductivity increased ratio in concentrated cell and the solution conductivity decreased ratio in concentrated cell, are used to evaluate the desalination property in ED.

As shown in Fig. S3, in dilute cell, the separation factors is the solution conductivity decreased ratio,

$$S_F = \frac{c_0 - c_t}{c_0} = 1 - \frac{c_t}{c_0}$$

in dilute cell, the separation factors is the solution conductivity increased ratio,

$$S_F = \frac{c_t - c_0}{c_0} = \frac{c_t}{c_0} - 1$$

$$c_i \propto \sigma$$

Where c_0 is the concentration of initial solution; c_t is the concentration of solution at the time of t; σ is the conductivity of solution.

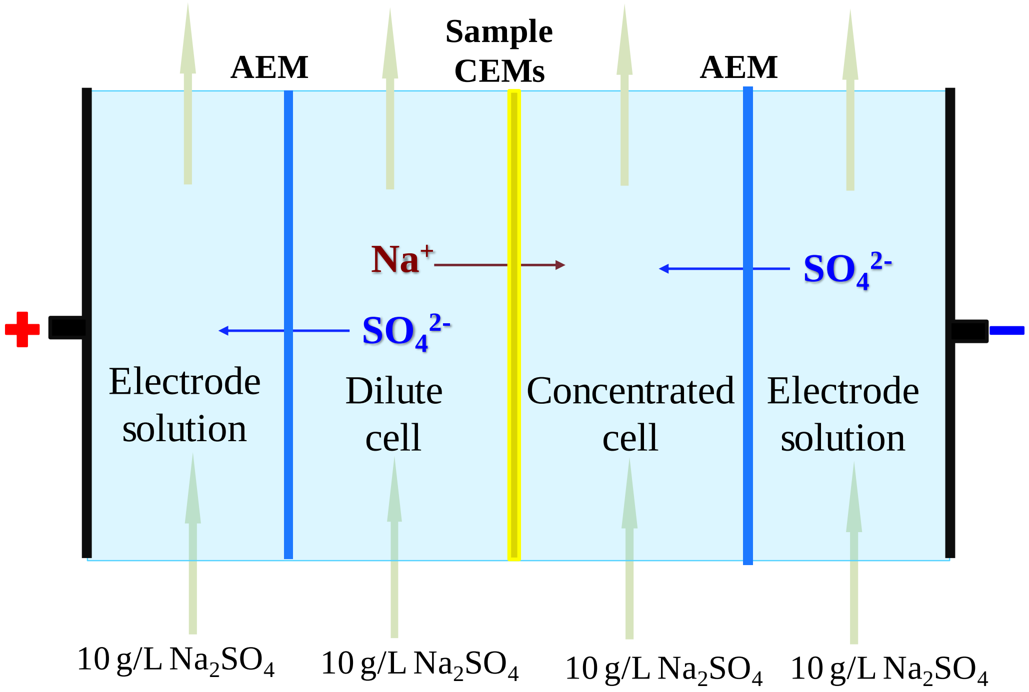

Fig. S3 Schematic diagram of desalination in ED.

2. Materials

Kevlar aramid nanofibers were obtained from Zhangjiagang Free Trade Zone Fengduo International Trade Co., Ltd., (Zhangjiagang, China). Potassium hydroxide (KOH, 85%) in the form of pellets was obtained from Acros Organics NV. Dimethyl sulfoxide (DMSO, 99.5%) was obtained from VWR International BVBA. 1-ethyl-3-(3-dimethylami-nopropyl) carbodiimide hydrochloride (EDC-HCl), 4-amino-benzenesulfonic acid (ABS), and N-hydroxy succinimide (NHS) were purchased from Aladdin Industrial Co. Ltd. (China). Sodium hydrogen oxide (NaOH), hydrochloride acid (HCl), sodium chloride (NaCl), sodium sulfate (Na_2SO_4) and all other chemicals were obtained from Sigma-Aldrich (Germany), and all the chemicals were used without any further purification. The commercial original AEM (Type I) were the homogeneous membranes and purchased from FUJIFILM Manufacturing Europe B.V. (Japan).

3. Methods

3.1. Preparation of membrane casting solution.

2% (quality ration) Kevlar aramid nanofibers, 3% KOH and 95% DMSO were mixed in the glass media storage bottles with magnetic stirring. 10 days later, membrane casting solution then obtained after deaeration treatment for 10 hours, as shown in Fig. S4.

Fig. S4. Schematic diagram of preparation of membrane casting solution.

3.2. Preparation of the Kevlar cation exchange membranes.

Firstly, the casting solutions were poured onto a clean glass plate, then using a casting knife set to a thickness of 250 μm at 25 ℃. Then, the glass plate was immediately immersed into pure water and the Kevlar gel membrane was produced via phase inversion.

15 min later, the membranes were carefully peeled off from the glass plate and transferred to the 1 L ABS solution (different concentrations of ABS) with 1g EDC ~~H~~Cl and 0.6 g NHS solution.

Sever days later (time of amide condensation reaction), the membranes were carefully cleaned by pure water for five times and put on the surface of non-woven polypropylene fabric.

Then, the as-prepared gel membranes were dried in an oven at 65 ℃ by air dry oven for 8 hours (Be careful! In this step, both side of the as-prepared gel membrane should be fixed by using non-woven polypropylene fabrics to avoid the shrinkage of gel membranes).

Finally, the resulting membranes were obtained.

3.3. Measurement of ion exchange capacity of membranes.

Ion exchange capacity (IEC) is crucial electrochemical property of in exchange membranes, which is measured by acid-base titration method. In this work, the dry Kevlar CEMs were weighed (m_{dry}) and measured into 1 M HCl for 48h. Then, the Kevlar CEMs were washed 3 times by pure water and make sure there was no absorbed HCl on the surface of Kevlar CEMs. Then the Kevlar CEMs was immersed in 0. 5 M NaCl for 48 h. The solution was titrated by using 0.01 M NaOH and phenolphthalein as indicator. The IEC value was calculated from the measured amounts of exchanged H^+ and the IEC was calculated by

$$\mathrm{IEC} = \frac{(V_s - V_b) \cdot c_{NaOH}}{m_{dry}}$$

where V_s is the volume of consumed NaOH by membranes; V_b is the volume of consumed NaOH without membranes and c_{NaOH} is the concentration of NaOH; m_{Dry} is the weight of the dry membranes.

3.4. Measurement of water content of membranes.

The water content of the membranes was calculated by measuring the change of weight before and after hydrating. Prior to the measurement, the absolute dry membrane was obtained by drying the samples in a vacuum oven at 60 ℃ for 12 h. After that, the membrane samples were immersed in water and the change of weight was measured and calculated as

$$\mathrm{W}(\%)=\frac{\mathrm{m_{Wet}}-\mathrm{m_{Dry}}}{\mathrm{m_{Dry}}}\times 100\% \qquad (3)$$

where $\mathrm{m_{Wet}}$ is the weight of wet membrane samples, $\mathrm{m_{Dry}}$ is the weight dry membrane samples.

3.5. Measurement of swelling rate of membranes.

The swelling rate of membranes was calculated by measuring the change of length when being hydrated. Prior to the measurement, the absolute dryness of membrane samples were obtained by drying in a vacuum oven at 60 ℃ for 12 h. After that, the membrane samples were immersed in water and the change of length and calculated as

$$\mathrm{S}(\%)=\frac{\mathrm{L_{Wet}}-\mathrm{L_{Dry}}}{\mathrm{L_{Dry}}}\times 100\% \qquad (4)$$

where $\mathrm{L_{Wet}}$ is the length of wet membrane samples, $\mathrm{L_{Dry}}$ is the length of dry membranes.

3.6. Measurement of membrane surface electric resistance

As shown in Fig. S5, the membrane surface electrical resistance was measured in a 0.50 M NaCl solution, 0.2 M Na2SO4 was chosen as the electrode solution. The surface electrical resistance R_{SER} ($\Omega\cdot cm^2$) was calculated as

$$R_{SER} = \frac{U - U_0}{I} \times S$$

where U is the voltage of the membranes and U_0 is the voltage of the blank expressed in V, I is the constant current through the membranes, which was 0.04 A. S is the effective area of the membrane, which was 7.065 cm^2.

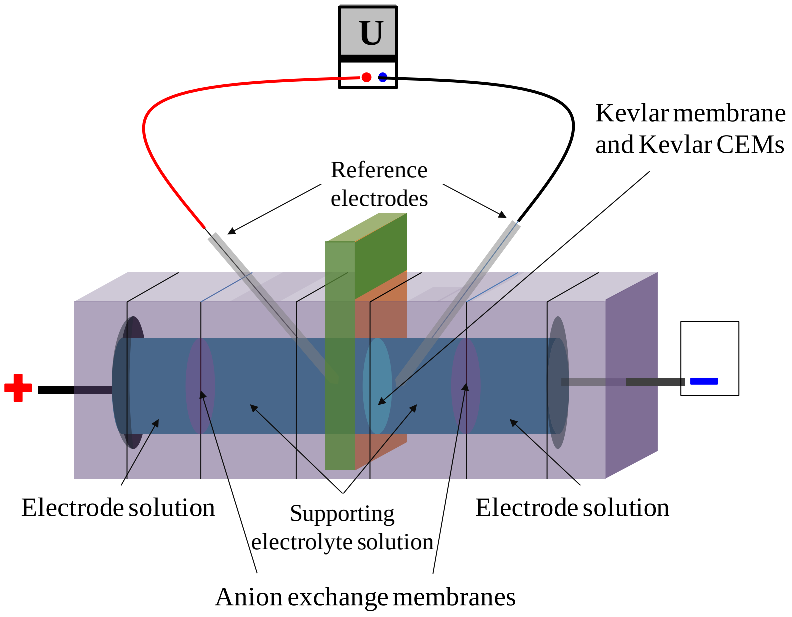

Fig. S5 The membrane surface electric resistance measurement (also used for polarization current-voltage curve measurement).

3.7. Measurement of the membrane zeta potential.

The zeta potential of the membranes were measured by using a SurPASS™ 3 electro-kinetic analyzer (Anton Paar, Graz, Austria). Membrane samples were washed and rinsed in pure water for 24 hours before measuring. The zeta potential was determined in a background electrolyte of 1 mM KCl solution over a pH range from 3.0 to 10.0 at room temperature.

3.8. Measurement of the current-voltage curves of all the Kevlar CEMs.

As shown in Figure S5, the polarization current voltage curves were measured in a four-electrode mode under direct current to characterize the electrochemical behavior of the modified membranes. 0.1 M NaCl and 0.5 M Na_2SO_4 were used as test solution and electrode solution respectively. The effective area of membrane was 7.065 cm^2.

3.9. Total reflectance Fourier transforms infrared (ATR-FTIR).

Total reflectance Fourier transform infrared spectroscopy (ATR-FTIR, Nicolet 6700, United States) was used to monitored the change of the functional groups of membrane surface. Membranes were dried thoroughly in vacuum oven at 45 ℃ for 12 h before measurements.

3.10. Scanning electronic microscopy (SEM)

The morphologies and structures of Kevlar membrane and Kevlar CEMs (surface and cross-sectional) were characterized by using scanning electronic microscopy (SEM, Hitachi S-4800) at an accelerating voltage of 10.0 kV.

3.11. X-ray photo-electron spectroscopy (XPS).

The elemental compositions of the membranes were analyzed by X-ray photo-electron spectroscopy (XPS, Kratos AXIS Ultra DLD, Japan). The anode was mono (Al (Mono)) (45 W). The charge neutralizer was on current 1.8 A, balance 3.3 V and bias 1.0 V.

3.12. The mechanical properties of the membrane.

In this work, the mechanical strength of the thin membranes (thickness are about 5 μm) was characterized by a glass-tube column (height 90.0 cm and diameter 1.5 cm, shown in Fig. S6a and Fig. S6b). The resulting membranes were stuck onto the edge of glass-tube column, shown in Fig. S6c. Then, the withstand pressure (p, kPa) of membrane was calculated as

$$p = \rho g h$$

where ρ is the density of water, which is 0.997g/L. g is the gravitational acceleration (~ 9.8 N/kg); h is the height of water column and expressed in m.

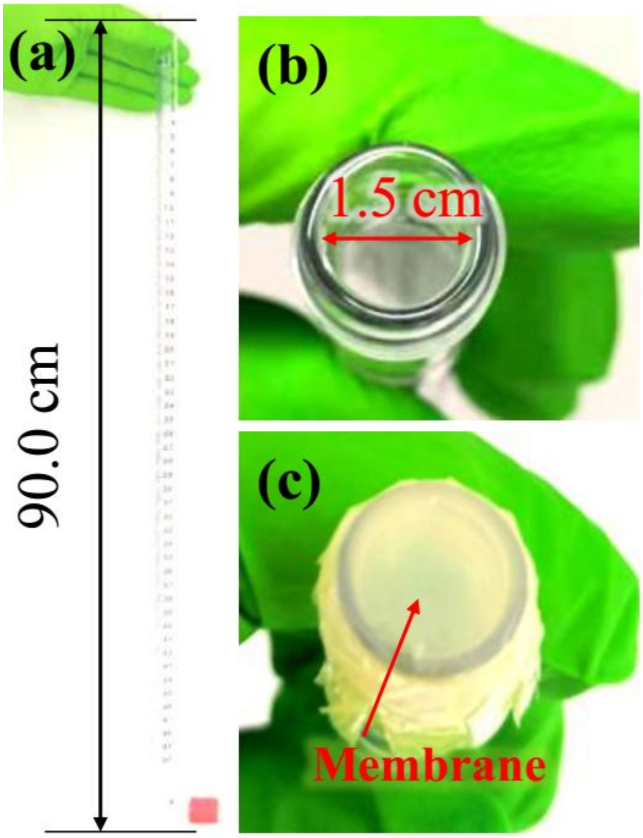

Fig. S6 The mechanical strength of the thin membranes measurement, the height (a) and diameter (b) of the glass-tube column, and the resulting membranes were stuck onto the edge of glass-tube column (c).

3.13. Desalination of the membranes

Fig. S6 shows the lab-design desalination device, the Kevlar CEM samples are put in the middle of the device, and two anion exchange membrane are set on the both side of the device. In desalination, 10 g L^{-1} Na_2SO_4 were chosen as the electric solution and electrolyte solutions in both dilute cell and concentrated cell. Every 5 min, measuring the conductivities in both dilute and concentrated cells.

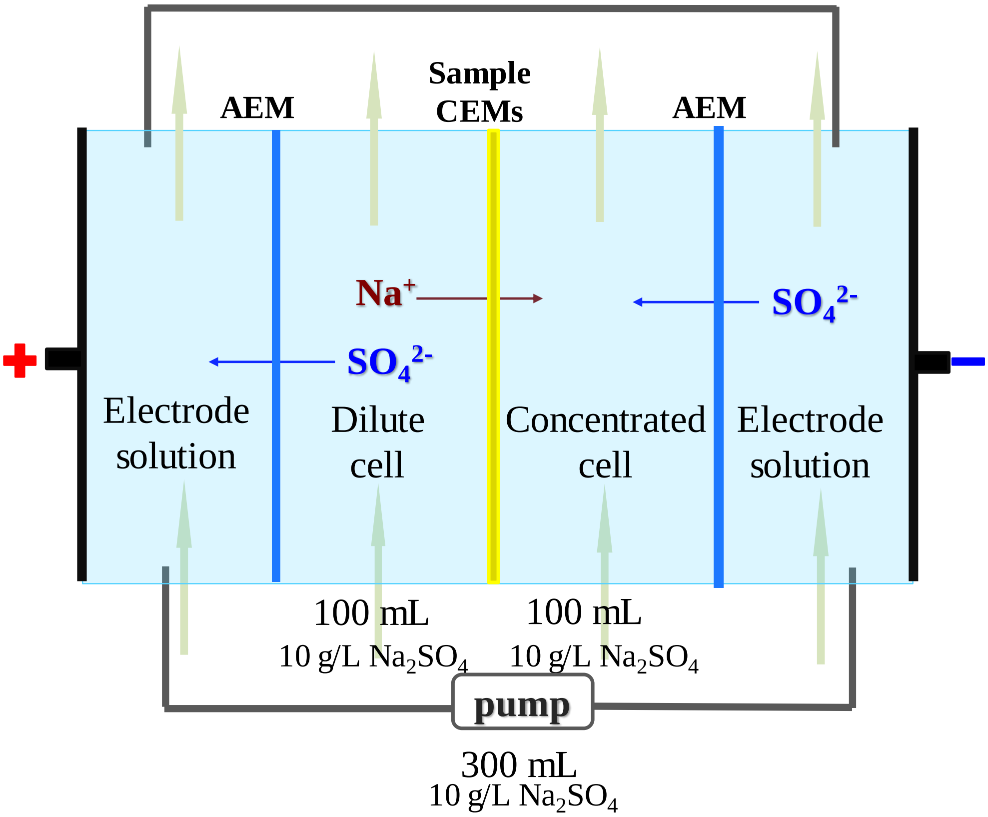

Fig. S7 The lab-design desalination device.

3.14. Organic solvent property measurement.

The Kevlar CEM-3 were selected as the membrane sample and measuring into 25%, 50%, 75% and 100% ($V_{acetone}/V_{water}$) aqueous acetone solutions for 72 h. After that, measuring the desalination property as the above steps.

4. Results.

4.1. Attenuated total reflectance Fourier transform infrared spectroscopy.

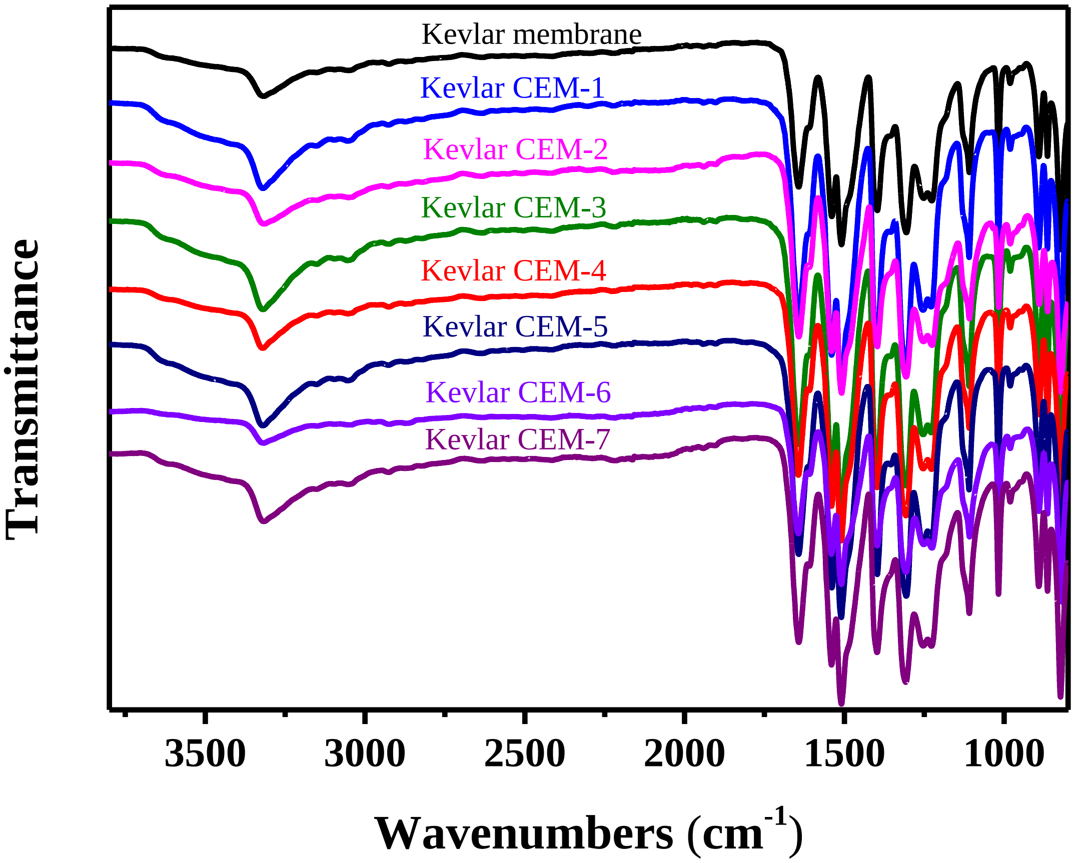

Fig. S8 The ATR-FTIR of membranes.

4.2. X-ray photoelectron spectroscopy

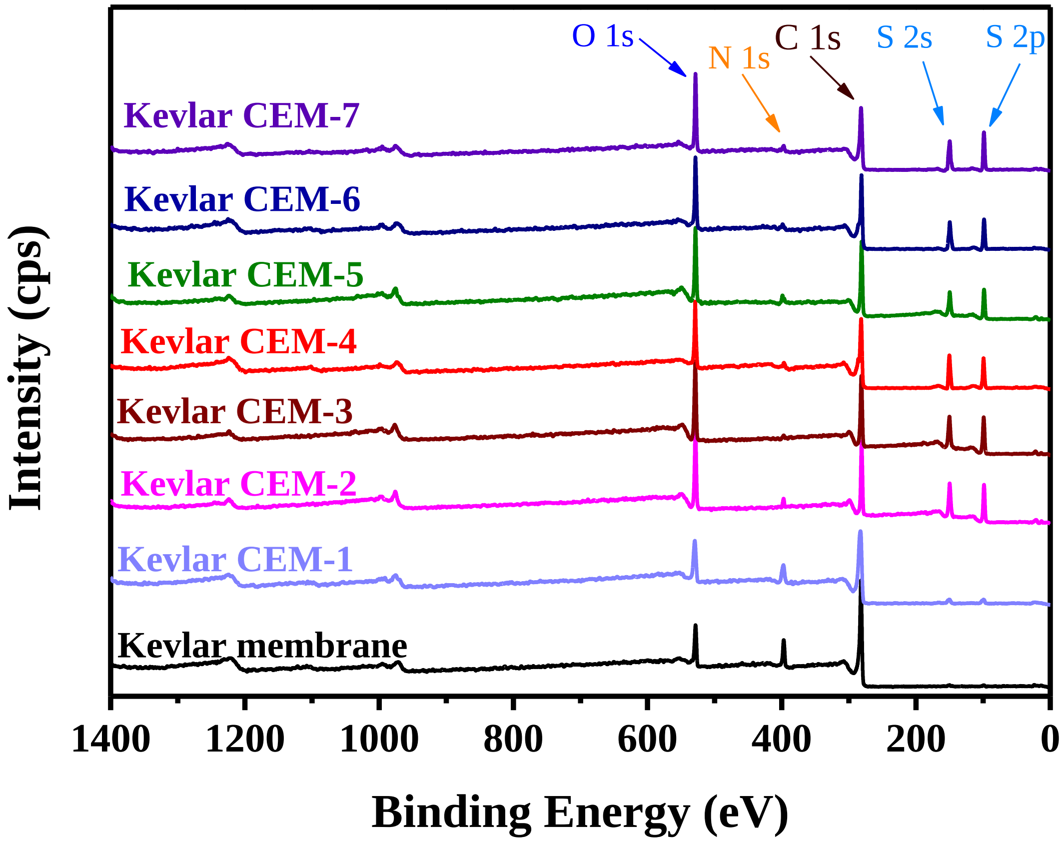

Fig. S9 The XPS of membranes.

4.3. Polarization current-voltage curves.

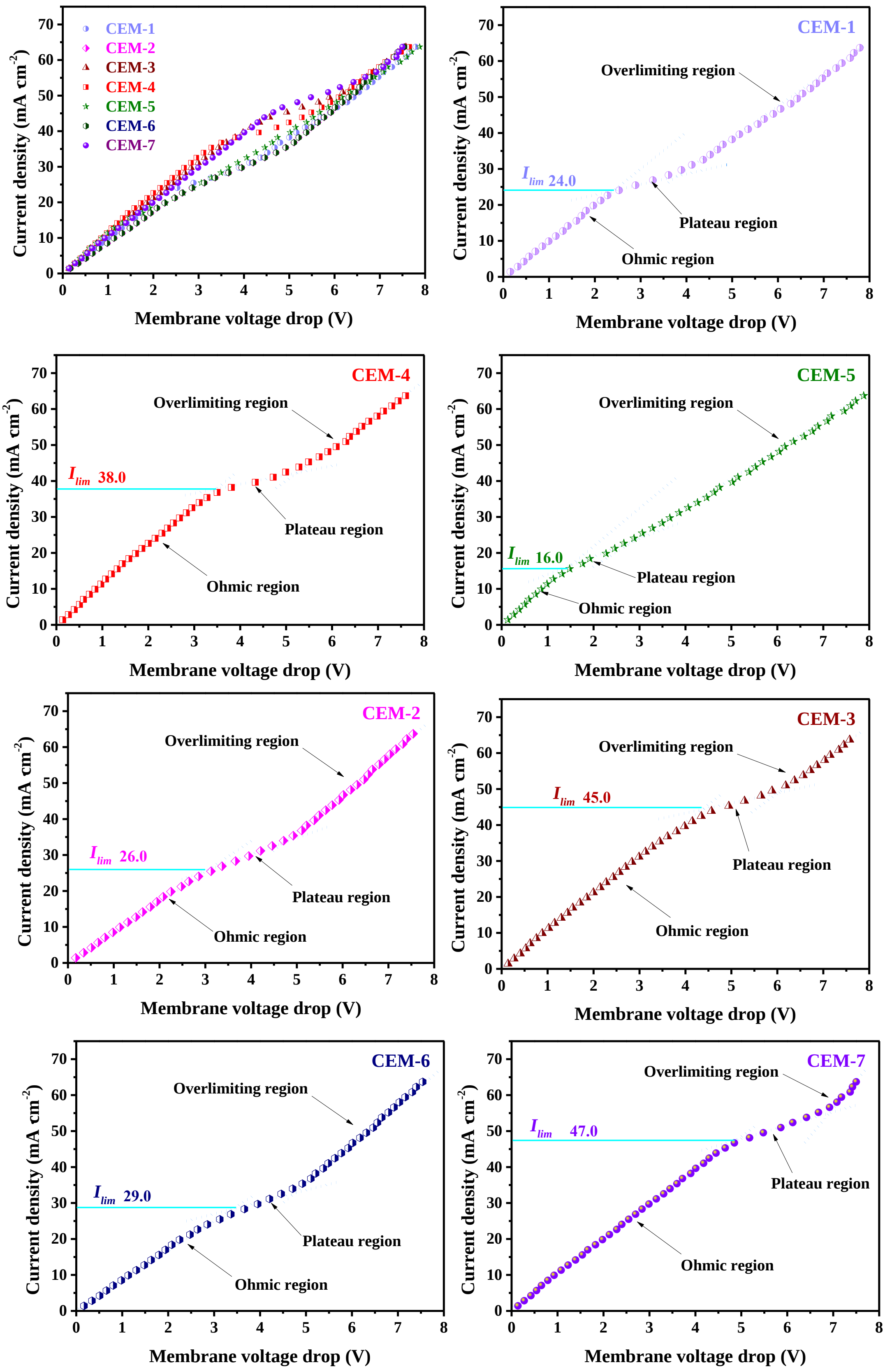

Fig. S10 Polarization current-voltage curve of membranes.

4.4. Scanning electronic microscopy of membrane surface.

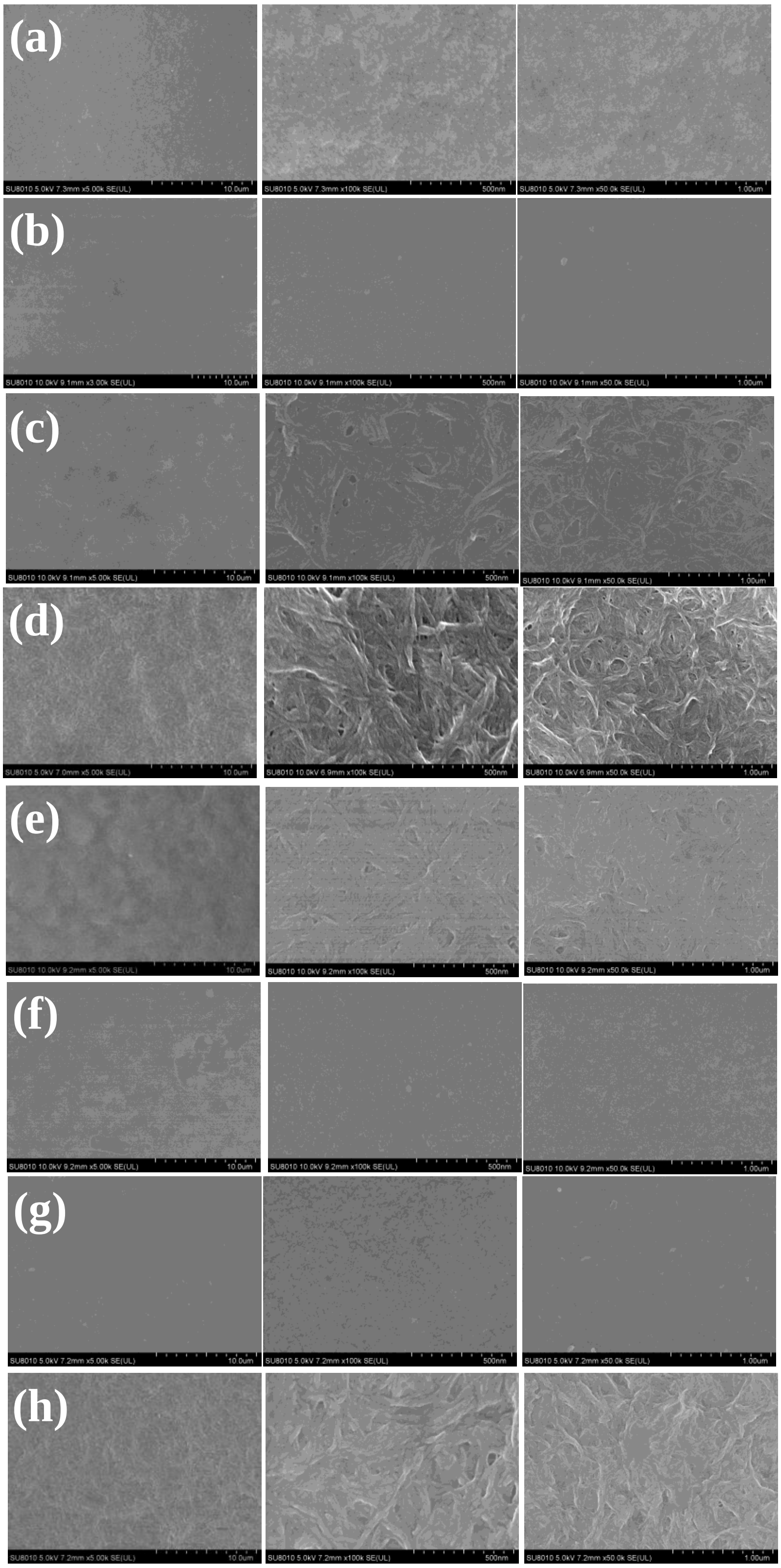

Fig. S11. SEM images of membrane surface, Kevlar membrane (a), Kevlar CEM-1 (b), Kevlar CEM-2 (c), Kevlar CEM-3 (d), Kevlar CEM-4 (e), Kevlar CEM-5 (f), Kevlar CEM-6 (g) and Kevlar CEM-7 (h).

4.5. Desalination.

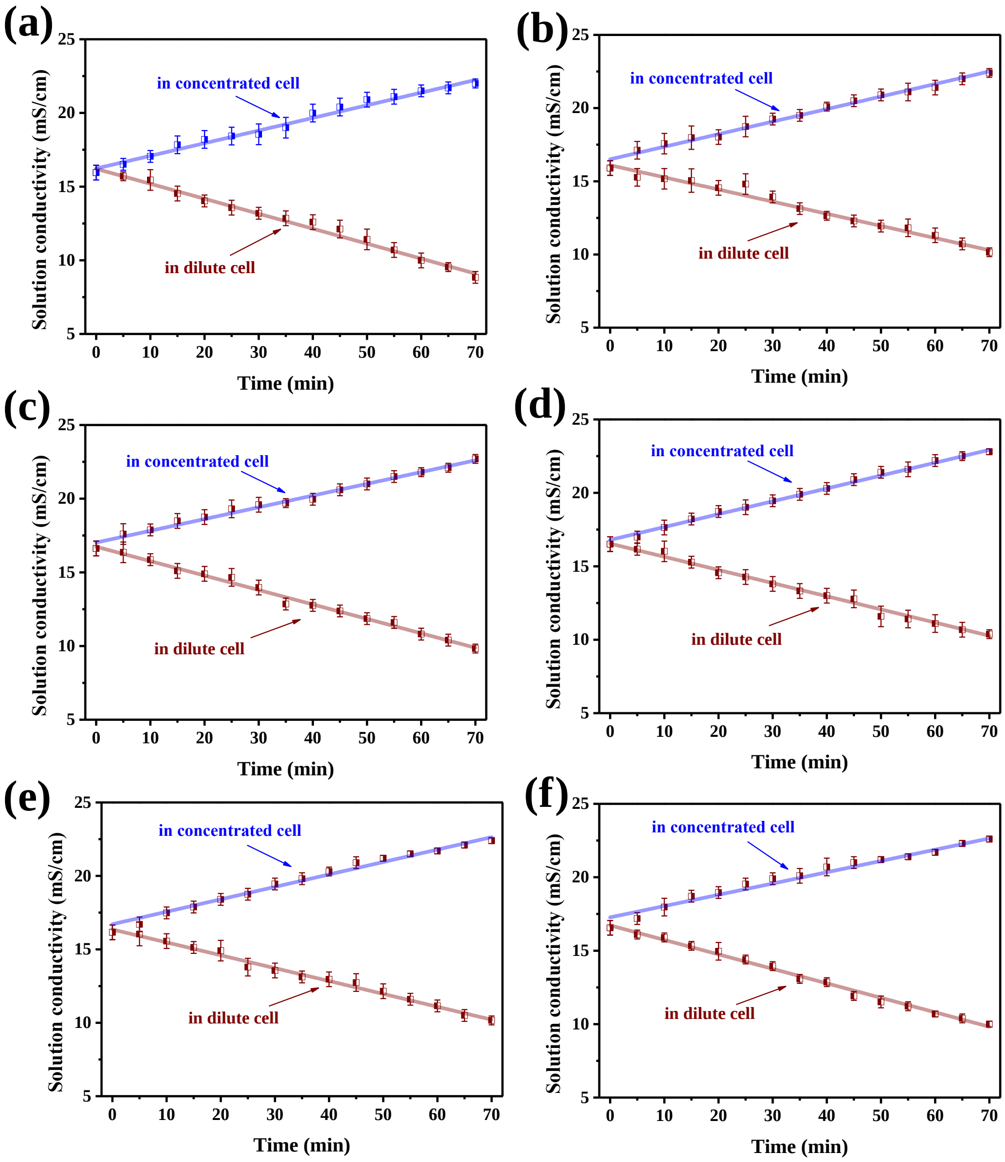

Fig. S12. In desalination, the solution conductivity changed of Kevlar CEM-1 (a), Kevlar CEM-2 (b) Kevlar CEM-4 (c) Kevlar CEM-5 (d) Kevlar CEM-6 (e) and Kevlar CEM-7 (f), in concentrated and dilute cells, respectively.

4.6. The equation of liner fit for Kevlar CEMs in desalination.

Equation: $y = a + b \cdot x$

Table S1. The equation of liner fit for Kevlar CEM-1 in desalination of 10 g L^{-1} Na_2SO_4.

Cells	Intercept (a)	Slope (b)
Dilute	16.00516	-0.08159
Concentrated	16.22604	0.08484

Table S2. The equation of liner fit for Kevlar CEM-2 in desalination of 10 g L^{-1} Na_2SO_4.

Cells	Intercept (a)	Slope (b)
Dilute	16.09691	-0.08299
Concentrated	16.49969	0.08574

Table S3. The equation of liner fit for Kevlar CEM-3 in desalination of 10 g L^{-1} Na_2SO_4.

Cells	Intercept (a)	Slope (b)
Dilute	16.96393	-0.09338
Concentrated	16.88736	0.08887

Table S4. The equation of liner fit for Kevlar CEM-4 in desalination of 10 g L^{-1} Na_2SO_4.

Cells	Intercept (a)	Slope (b)
Dilute	16.7391	-0.09799
Concentrated	17.02002	0.07972

Table S5. The equation of liner fit for Kevlar CEM-5 in desalination of 10 g L^{-1} Na_2SO_4.

Cells	Intercept (a)	Slope (b)
Dilute	16.54219	-0.09199
Concentrated	16.79307	0.08772

Table S6. The equation of liner fit for Kevlar CEM-6 in desalination of 10 g L^{-1} Na_2SO_4.

Cells	Intercept (a)	Slope (b)
Dilute	16.34981	-0.08774
Concentrated	16.70789	0.08747

Table S7. The equation of liner fit for Kevlar CEM-7 in desalination of 10 g L^{-1} Na_2SO_4.

Cells	Intercept (a)	Slope (b)
Dilute	16.71921	-0.0986
Concentrated	16.96737	0.08768

4.7. The equation of liner fit for Kevlar CEMs in desalination after measuring the organic solvent property.

Table S8. The equation of liner fit for Kevlar CEM-3 in desalination of 10 g L^{-1} Na_2SO_4 after the treatment of measuring in 25% acetone.

Cells	Intercept (a)	Slope (b)
Dilute	15.7354	-0.08262
Concentrated	15.9391	0.08069

Table S9. The equation of liner fit for Kevlar CEM-3 in desalination of 10 g L^{-1} Na_2SO_4 after the treatment of measuring in 50% acetone.

Cells	Intercept (a)	Slope (b)
Dilute	15.58557	-0.07581
Concentrated	16.30312	0.0638

Table S10. The equation of liner fit for Kevlar CEM-3 in desalination of 10 g L^{-1} Na_2SO_4 after the treatment of measuring in 75% acetone.

Cells	Intercept (a)	Slope (b)
Dilute	16.2853	-0.07534
Concentrated	16.96653	0.05853

Table S11. The equation of liner fit for Kevlar CEM-3 in desalination of 10 g L^{-1} Na_2SO_4 after the treatment of measuring in 100 % acetone.

Cells	Intercept (a)	Slope (b)
Dilute	16.72094	-0.07543
Concentrated	17.24575	0.0605

5. References

1. Z. Tan, S. Chen, X. Peng, L. Zhang and C. Gao, *Science*, 2018, **360**, 518-521.
2. Y. Zhao, Y. Li, S. Yuan, J. Zhu, S. Houtmeyers, J. Li, R. Dewil, C. Gao and B. Van der Bruggen, *J. Mater. Chem. A*, 2019, **7**, 6348-6356.
3. F.-M. Allioux, S. Balme and L. F. Dumée, *Mater. Horiz.*, 2018, **5**, 1185-1193.
4. Y. Zhao, K. Tang, H. Liu, B. Van der Bruggen, A. Sotto Díaz, J. Shen and C. Gao, *J. Membrane Sci.*, 2016, **520**, 262-271.
5. T. Xu, *J. Membrane Sci.*, 2005, **263**, 1-29.
6. Y. Zhao, J. Zhu, J. Li, Z. Zhao, S. I. Charchalac Ochoa, J. Shen, C. Gao and B. Van der Bruggen, *ACS Appl. Mater. Interfaces*, 2018, **10**, 18426-18433.
7. C. Klaysom, B. P. Ladewig, G. Q. M. Lu and L. Wang, *J. Membrane Sci.*, 2011, **368**, 48-53.
8. F. Xu, C. Innocent and G. Pourcelly, *Sep. Purif. Technol.*, 2005, **43**, 17-24.
9. I. Soroko, Y. Bhole and A. G. Livingston, *Green Chem.*, 2011, **13**, 162-168.
10. D. Li, X. Gou, D. Wu and Z. Guo, *Nanoscale*, 2018, **10**, 6695-6703.
11. S. Yuan, J. Swartenbroekx, Y. Li, J. Zhu, F. Ceyssens, R. Zhang, A. Volodine, J. Li, P. Van Puyvelde and B. Van der Bruggen, *J. Membrane Sci.*, 2019, **573**, 612-620.
12. Y. Li, S. Yuan, C. Zhou, Y. Zhao and B. Van der Bruggen, *J. Mater. Chem. A*, 2018, **6**, 22987-22997.
13. Y. Zhao, W. Shi, B. Van der Bruggen, C. Gao and J. Shen, *Adv. Mater. Interfaces*, 2018, **5**, 1701449.
14. Y. Zhao, C. Zhou, J. Wang, H. Liu, Y. Xu, J. W. Seo, J. Shen, C. Gao and B. Van der Bruggen, *J. Mater. Chem. A*, 2018, **6**, 18859-18864.
15. Y. Zhao, K. Tang, H. Ruan, L. Xue, B. Van der Bruggen, C. Gao and J. Shen, *J. Membrane Sci.*, 2017, **536**, 167-175.
16. Y. Zhao, J. Zhu, J. Ding, B. Van der Bruggen, J. Shen and C. Gao, *J. Membrane Sci.*, 2018, **548**, 81-90.
17. I. Soroko, M. P. Lopes and A. Livingston, *J. Membrane Sci.*, 2011, **381**, 152-162.
18. Y. Zhao, C. Gao and B. Van der Bruggen, *Nanoscale*, 2019, **11**, 2264-2274.
19. H. Niu, Y. Zhang, Y. Liu, B. Luo, N. Xin and W. Shi, *J. Mater. Chem. A*, 2019.
20. Y. Liu, X. Gao, Z. Hong and W. Shi, *J. Mater. Chem. A*, 2016, **4**, 8983-8988.
21. L. Fan, K. Lin, J. Wang, R. Ma and B. Lu, *Adv. Mater.*, 2018, **30**, e1800804.